

Termination of the series of fractional quantum Hall states at small filling factors

R. L. Willett

Massachusetts Institute of Technology, Cambridge, Massachusetts 02139

H. L. Stormer

AT&T Bell Laboratories, Murray Hill, New Jersey 07974

D. C. Tsui

Department of Electrical Engineering, Princeton University, Princeton, New Jersey 08540

L. N. Pfeiffer, K. W. West, and K. W. Baldwin

AT&T Bell Laboratories, Murray Hill, New Jersey 07974

(Received 17 June 1988)

We report magnetotransport measurements on low-density, high-mobility two-dimensional (2D) electron systems in (Al,Ga)As/GaAs heterostructures down to Landau-level filling factors of $\nu \sim \frac{1}{18}$. We observe a striking activated temperature dependence with onset near $\nu \sim \frac{1}{5}$ and continuing to smallest ν . The activation energy increase is approximately linear with decreasing ν and its slope depends monotonically on 2D density. While magnetic-field-induced localization cannot be ruled out, several features of the results are consistent with the formation of a pinned 2D Wigner crystal.

There exists overwhelming evidence that the fractional quantum Hall effect¹ (FQHE) is a result of two-dimensional (2D) electron condensation into incompressible quantum fluids at Landau-level filling factors $\nu = 1/m$, well described by Laughlin's many-particle wave function.² Subsequently discovered FQHE characteristics at $\nu = p/q$ are believed to be correlated ground states of quasiparticles derived from the primitive $1/m$ fluids.³ This hierarchy of daughter states comprises all odd-denominator rational fractions. The question as to the termination of the hierarchy arises naturally. Sufficient disorder is expected to terminate each sequence by localizing lower-level quasiparticles preventing them from forming the next level correlated ground state.⁴ Alternatively, crystallization into a 2D Wigner solid,^{5,6} probably pinned to residual defects, is postulated for low-disorder specimens. Such an ordered state remains unobserved.

Manifestation of a Wigner lattice is expected to be best observed in the termination of the primitive sequence $\nu = 1/m$ in the small- ν limit. Lam and Girvin⁷ have proposed a transition at ν slightly larger than $\frac{1}{7}$, using a variational wave function and including particle correlations. Levesque, Weis, and MacDonald⁸ find a liquid-to-crystal transition at $\nu < \frac{1}{9}$. More recently Girvin, MacDonald, and Platzman⁹ formulated the magnetoroton theory of collective excitations in the FQHE. The energy gap approaches zero at the magnetoroton minimum for $\nu = \frac{1}{7}$, indicating its proximity to another phase.

These model calculations have seen little testing in experiments due to the difficulty of examining 2D systems at small ν . An early measurement¹⁰ on a moderate mobility ($\mu \sim 4 \times 10^5$ cm²/V sec) GaAs/(Al,Ga)As heterostructure down to $\nu = \frac{1}{11}$ at $T = 0.51$ K obtained a weak inflection in ρ_{xx} at $\nu = \frac{1}{5}$ but no distinctive transport features were resolved at smaller ν . Higher-mobility samples have since

produced well developed $\nu = \frac{1}{5}$ minima, but meaningful transport data could not be obtained for smaller ν at lower T probably due to deteriorating electrical contact to the 2D system with increasing magnetic field.

With our recent (Al,Ga)As/GaAs heterostructures, we have overcome most of these experimental difficulties and are able to conduct transport experiments at filling factors as small as $\nu \sim \frac{1}{18}$. At low temperatures we observe a striking increase in Hall and longitudinal resistivities with onset near $\nu = \frac{1}{5}$ and extending throughout the observable range of smaller ν . The precise filling factor at which these resistivity deviations have their onset depends on the 2D carrier density. The temperature dependence of ρ_{xx} is activated throughout the small filling factor regime. The activation energies were found to be density dependent and to increase with decreasing filling factor. We discuss these results with respect to magnetic localization or Wigner crystallization as possible explanations.

Our single-interface GaAs/(Al,Ga)As samples contained a 2000-Å setback layer between the GaAs/(Al,Ga)As interface and the silicon-sheet-doped layers. Several samples from two different wafers were measured with similar results. Low-temperature illumination for several minutes with a light-emitting diode produced the persistent photocarriers with an areal density of $n \sim 3 \times 10^{10}$ cm⁻² and mobility $\mu \sim 1.2 \times 10^6$ cm²/V sec. The areal density could be increased to $n \sim 5 \times 10^{10}$ cm⁻² and $\mu \sim 1.7 \times 10^6$ cm²/V sec by application of a backside gate voltage. Transport measurements were made using low-frequency (< 5 Hz) and low-amplitude (< 10 nA) excitation currents. A dilution refrigerator provided temperatures down to 80 mK in magnetic fields up to 31 T. The samples were submerged in He³-He⁴ mixture adjacent to a calibrated carbon resistor with known magnetoresistance.

Figure 1 shows Hall and longitudinal resistivities at four different temperatures. A marked increase in resistance with decreasing temperature is apparent in both ρ_{xx} and ρ_{xy} at high B fields. The onset of the strong T dependence in ρ_{xx} occurs at a single magnetic field value for all traces over the entire temperature range investigated, $80 < T < 800$ mK. The onset in ρ_{xy} appears at a slightly larger magnetic field at $\nu \sim \frac{1}{3}$ in the sample displayed.

The ρ_{xx} and ρ_{xy} traces are terminated at high fields by a noisy resistance roll-off which marks the onset of large, out-of-phase components. The signal deterioration prohibits concurrent very high B and very low T measurements. Its origin remains uncertain. Mixing of ρ_{xx} into ρ_{xy} often poses a problem in magnetotransport measurements. Admixtures of ρ_{xx} to ρ_{xy} due to contact misalignment can be compensated by averaging data from measurements with opposite B direction. At present there exists no scheme to assess mixing of ρ_{xx} into ρ_{xy} due to sample inhomogeneities. Reversed-field experiments on our samples reproduce ρ_{xx} but differ significantly in ρ_{xy} , and consequently we cannot rule out that the T dependence of ρ_{xy} is not caused by admixtures of ρ_{xx} to ρ_{xy} . Therefore, we concentrate on the ρ_{xx} data.

Figure 2(a) shows ρ_{xx} vs $1/T$ on a semilogarithmic scale for several magnetic field values. ρ_{xx} displays strikingly activated behavior over almost two decades. We

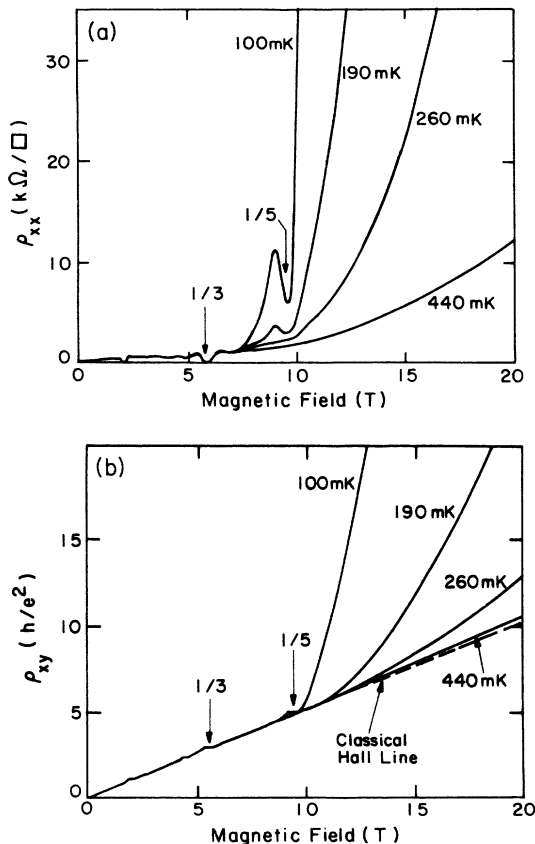


FIG. 1. (a) Diagonal resistivity ρ_{xx} and (b) Hall resistance ρ_{xy} of a low-density ($n = 4.8 \times 10^{10} \text{ cm}^{-2}$) high-mobility ($\mu = 1.7 \times 10^6 \text{ cm}^2/\text{V sec}$) two-dimensional electron system at various temperatures.

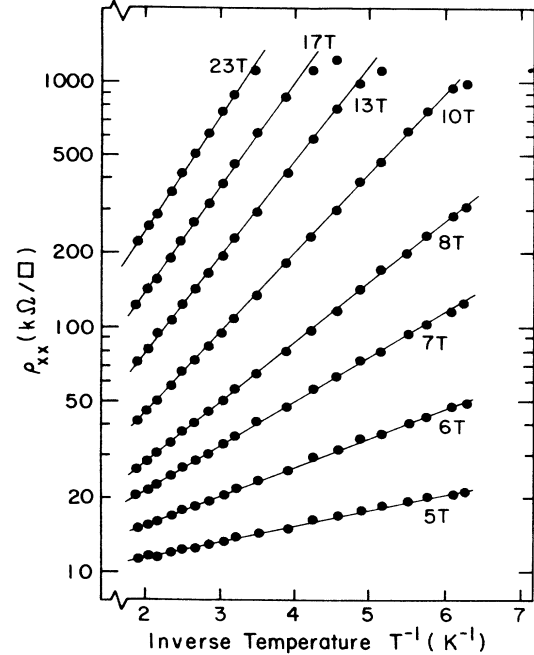


FIG. 2. Temperature dependence of diagonal resistivity ρ_{xx} at eight different magnetic fields at density $3 \times 10^{10} \text{ cm}^{-2}$.

determined the activation energies E_A from Fig. 2 according to $\rho_{xx} = \rho_0 \exp(E_A/2T)$.

Our most important result is shown in Fig. 3, where E_A is plotted versus ν for three different densities. The data stretch over a very large range of Landau-level filling, $0.04 < \nu < 0.3$, approaching the classical limit as $\nu \rightarrow 0$, $B \rightarrow \infty$, and the magnetic length $l_0 \rightarrow 0$. E_A vs ν is roughly linear with some deviation at $\nu = 0.20$ ($= \frac{1}{5}$). Its intercept with the horizontal axis marks the onset of the temperature dependence. As the density is increased, this threshold shifts to smaller filling factor, and the slope increases leading to a larger extrapolated activation energy $E_A(\nu=0)$. The data seem to have a common intercept at $\nu \sim 0.19$.

We consider two possible origins for the results of Fig. 3: magnetic-field-induced carrier localization or formation of a Wigner lattice which is pinned to residual disorder sites. The present theoretical models of localization and Wigner crystallization do not elaborate their respective transport properties. Consequently, the interpretation of our results can only rely on comparison to the general characteristics of these models.

From the mobility we can estimate a Landau-level broadening $\Gamma = \hbar/\tau \approx 1 \text{ K}$, comparable to the activation energies of Fig. 3. To consider more quantitatively transport dominated by localization, we resort to the widely used single-particle picture of Landau-level broadening with activation to the delocalized states in the center of each Landau level. Assuming the width of the distribution to be B independent, and taking the experimental ν dependence of E_A to be linear, one arrives at a rectangular Landau level having width of twice $E_A(\nu=0)$ and a height about ten times larger than the zero-field density of states. Furthermore, about 50% of all states are delocal-

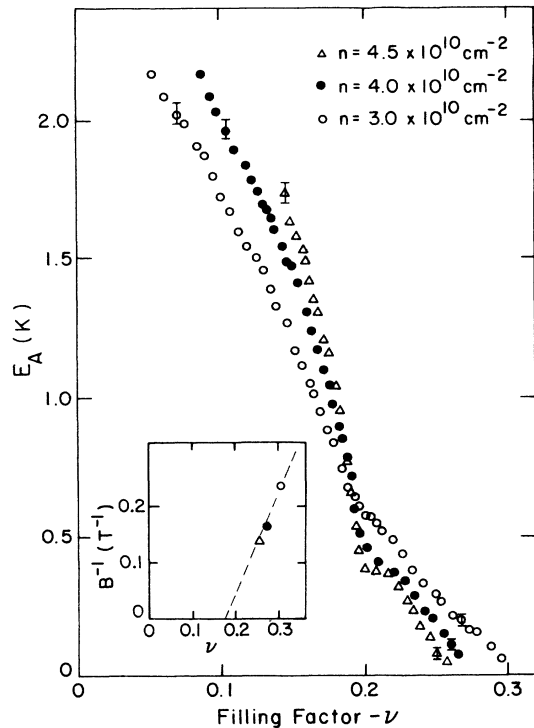


FIG. 3. Filling factor dependence of energy E_A at three different carrier densities. Inset shows extrapolation of onset $\nu(E_A=0)$ to infinite B using $\nu=nh/eB$.

ized at the center of the Landau level to account for the onset at $\nu \approx 0.25$. All this makes for an unlikely description of the density of states. However, several possible aspects of magnetic-field-induced localization may partially explain our data. In a simple picture of magnetic freeze-out, for a given density the activation energy E_A should be larger at higher B field and so E_A is expected to increase with decreasing ν . At a fixed ν , B is higher for higher n . Thus, E_A will be larger for higher n (as E_A is observed to be for $\nu \lesssim 0.19$ in our data). In addition, screening may be stronger for higher n , and so the onset of activation may be expected at smaller ν . This implies crossing of E_A vs ν for different n curves. A singular crossing point as observed at $\nu \approx 0.19$ in Fig. 3 would then be purely accidental. While this scenario is generally consistent with our data, one ultimately cannot conclude the role of localization in our results because the present theory of magnetic freeze-out is not sufficiently developed.

Formation of a pinned Wigner lattice represents an attractive alternate interpretation. The carriers condense into a solid phase due to strong electron-electron interaction.⁶ The lattice is pinned subsequently at random disorder sites, and electronic transport is dominated by thermal excitation. Elevation of electrons from the valence band of the Wigner solid to its lowest conduction band may pro-

vide such a mechanism. This energy gap¹¹ was calculated in Hartree-Fock to be $\sim 0.5e^2/\epsilon l_0$, which is ~ 100 K at 10 T and far exceeds our experimental energy scale. However, electron-electron correlation, finite thickness of the 2D system, Landau-level mixing, and residual disorder may drastically reduce this theoretical estimate. Other conduction mechanisms can also be postulated, such as thermal activation and dissociation of defect pairs in a Kosterlitz-Thouless¹² type of 2D melting. Activation energies for such defects are expected to be far below the single-particle Hartree-Fock results.

In the classical limit ($\nu \rightarrow 0$), from purely electrostatic considerations, all relevant energies scale as \sqrt{n} . The extrapolated values of $E_A(\nu=0)$ of Fig. 3 reflect such a monotonic increase of the characteristic energy as the density is raised.

Within a Wigner lattice model one can also reconcile the density dependence of the onset of activated behavior around $\nu \sim 0.27$ and, hence, the crossover of the data at $\nu \sim 0.19$. Starting from the FQHE, Wigner lattice formation can be regarded as a collapse of the quantum liquid gap and a freezing-in of the k vector associated with the roton minimum. Finite thickness of the 2D system and Landau-level mixing reduce this gap⁹ leading to a collapse at ν larger than $\nu \approx \frac{1}{7}$. Since lower electron densities require smaller magnetic fields to reach a given filling factor, Landau-level mixing is enhanced and Wigner lattice formation sets in at larger ν 's as observed in Fig. 3. Our data for the onset may be extrapolated in a crude fashion to infinite field values (assumed in all theoretical models) as shown in the inset of Fig. 3. A limiting value of $\nu \sim 0.19$ is reached for $B \rightarrow \infty$. Accepting the Wigner lattice interpretation, one can associate the three data points of the inset with a part of a phase boundary between an electron solid on the left and a rather complicated hierarchy of FQHE states on the right.¹³ Within this model it remains puzzling why the transport data show FQHE features at $\frac{1}{3}$ (and even $\frac{1}{7}$)¹⁴ within the solid part of the phase diagram.

In summary, we observe novel transport results in the small filling factor regime previously unexplored in such low-disorder systems. These phenomena may be explained by formation of a Wigner lattice or by single-particle localization.

We would like to thank J. P. Eisenstein, V. Elser, J. E. Furneaux, S. M. Girvin, R. P. Hall, C. Kallin, A. H. MacDonald, P. M. Platzman, and P. A. Wolff for helpful discussions and the staff of the Francis Bitter National Magnet Laboratory (FBNML) for valuable support. The FBNML was supported by the National Science Foundation (NSF). The work at Princeton University was supported by the NSF (Grant NO. DMR-8212167) and by the U.S. Office of Naval Research (Contract No. 00014-82-K-0450).

¹D. C. Tsui, H. L. Stormer, and A. C. Gossard, Phys. Rev. Lett. **48**, 1559 (1982).

²R. B. Laughlin, Phys. Rev. Lett. **50**, 1395 (1983).

³F. D. M. Haldane, Phys. Rev. Lett. **51**, 605 (1983).

⁴F. C. Zhang, Phys. Rev. B **34**, 5598 (1986).

⁵E. P. Wigner, Phys. Rev. **46**, 1002 (1934).

⁶Y. E. Lozovik and V. I. Yudson, Pis'ma Zh. Eksp. Teor. Fiz. **22**, 26 (1975) [JETP Lett. **22**, 11 (1975)].

- ⁷P. K. Lam and S. M. Girvin, Phys. Rev. B **30**, 473 (1984).
⁸D. Levesque, J. J. Weis, and A. M. MacDonald, Phys. Rev. B **30**, 1056 (1984).
⁹S. M. Girvin, A. M. MacDonald, and P. M. Platzman, Phys. Rev. Lett. **54**, 581 (1985); Phys. Rev. B **33**, 2481 (1986).
¹⁰E. E. Mendez, M. Heiblum, L. L. Chang, and L. Esaki, Phys. Rev. B **28**, 4886 (1983).
¹¹D. Yoshioka, and P. A. Lee, Phys. Rev. B **27**, 4986 (1983).
¹²J. M. Kosterlitz and D. J. Thouless, J. Phys. C **6**, 1181 (1973).
¹³P. M. Platzman, in *The Physics of the Two-Dimensional Electron Gas*, edited by T. J. Devreese and F. M. Peeters, NATO Advanced Study Institute, Ser. B, Vol. 157 (Plenum, New York, 1987), p. 87.
¹⁴V. J. Goldman, M. Shayegan, and D. C. Tsui, Phys. Rev. Lett. **61**, 881 (1988).